

A Kinetic and Surface Study of the Thermal Decomposition of Cellulose Powder in Inert and Oxidizing Atmospheres

C. FAIRBRIDGE, R. A. ROSS, and S. P. SOOD, *Department of Chemistry, Lakehead University, Thunder Bay, Ontario, Canada P7B 5E1*

Synopsis

The thermal decomposition of fibrous cellulose powder from 275° to 340°C has been studied by thermogravimetry, scanning electron microscopy, krypton adsorption, and gas-chromatographic analysis of the gaseous products arising from pyrolysis in various oxidizing and inert atmospheres. The reaction kinetics fit a phase boundary model where the rate is controlled by the movement of an interface through a cylindrical particle and the principal kinetic parameters fit a compensation curve described previously for the decomposition of wood products. An explanation of the physical mechanism of pyrolysis is proposed which is consistent with the observed rate data and the structural changes observed by scanning electron microscopy.

INTRODUCTION

In a recent publication,¹ kinetic and structural data obtained from a study of the pyrolysis of jack pine bark from 200° to 340°C were described. The physical mechanics of pyrolysis were interpreted on the basis of reaction initiation through the formation of planes of lateral strain which acted as decomposition sites decreasing in number inversely with time. The chemical significance of the hypothesis was obscured by the complex nature of the bark, and it was clear that an attempted elucidation of the process chemistry would depend on an evaluation of the nature of various reactions which might be expected to contribute to the overall pyrolysis. Since cellulose is a key component in such wood matrices, experiments on this material would aid in such an evaluation.

Previous related investigations of cellulose pyrolysis include isothermal studies in nitrogen,^{2,3} helium,⁴ and vacuum^{5,6,7,8}; and dynamic thermogravimetric analysis in nitrogen,⁹ vacuum,⁶ and air.¹⁰ Generally, the "activation energies" found by isothermal techniques are significantly lower than those derived from dynamic TG. Several workers^{4,5,6,11} noted first-order kinetic relationships which may signify that rate control in the systems studied could be associated with transport processes.

The present study of the thermal decomposition of cellulose powder has been carried out employing thermogravimetry, gas adsorption, scanning electron microscopy, and gas-chromatographic analysis of the gaseous products and elemental analysis of the residues on pyrolysis in various atmospheres.

Because there were few kinetic interpretations in the literature of cellulose pyrolysis in air, comparisons of pyrolysis phenomena in oxidizing as well as inert atmospheres were included. Isothermal experiments were conducted in the temperature range where active cellulose pyrolysis occurred.

EXPERIMENTAL

Materials

Whatman column chromedia CF1 fibrous cellulose powder (maximum 0.015% ash) was obtained from W. and R. Balston Ltd. and used as supplied.

Certified nitrogen, oxygen, helium, and compressed air were used as supplied by Canadian Liquid Air Ltd.

Apparatus and Procedure

The design and operating procedure of the Stanton-Redcroft Thermobalance and associated flow system have been described previously.¹ The flow rate of 230 ml/min (NTP) was chosen after tests which showed that the weight loss of 40-mg samples was independent of flow rate in the range of 150–500 ml/min (NTP).

Certified nitrogen (dried) and compressed air were used in the TG experiments conducted from ambient temperature to 1000°C at a heating rate of 7°C/min and in the isothermal weight change determinations conducted at temperatures from 298° to 341°C in nitrogen and 275° to 326°C in air. A saturator was used to introduce water vapor into the flowing nitrogen stream for some TG studies. The sample temperature, monitored by a thermocouple in the sample support in contact with the platinum crucible, rose to within 3°C of the selected isothermal temperature in less than 2 min, and constant temperature was achieved in less than 4 min.

Cellulose samples were characterized by krypton adsorption at -196°C and

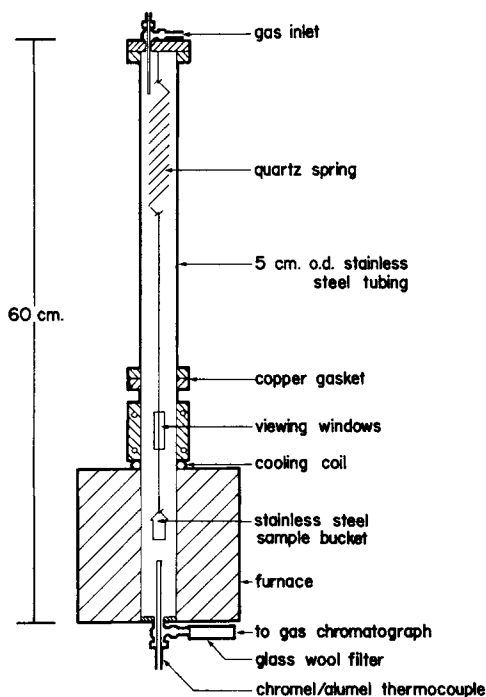


Fig. 1. Schematic of high-pressure apparatus.

by scanning electron microscopy using a Cambridge Stereoscan 600. Microscopy samples were coated with a thin layer of gold by a standard flash evaporation technique at 10^{-4} torr, and pictures were taken with a 35-mm camera attached to the CRT screen.

A stainless steel high-pressure apparatus, Figure 1, was used in conjunction with a Beckman GC-5 gas chromatograph to analyze the gaseous effluents from 100-mg cellulose samples. The gas chromatograph utilized Carbosieve B columns at 110°C with a helium flow rate of 30 ml/min (NTP). The effluent gases were analyzed by thermal conductivity detectors, and GC traces were recorded on a Beckman 10 in. recorder. Samples were weighed into the sample bucket, placed in the apparatus, and dried overnight in helium (6.5 atm) at 100°C . A GC trace was then obtained by flushing the gas sample through a sample loop. The apparatus was flushed with helium and repressurized. The temperature was then raised to a preselected value, and when sample weight was observed to decrease, a further GC trace was obtained. The apparatus was then purged and pressurized in preparation for the next run. A second series of experiments was conducted in a helium/oxygen (4/1 v/v) atmosphere at 6.5 atm. In order to separate O_2 and CO , the column temperature was programmed from 55° to 120°C . An in-line glass wool plug was installed at the gas outlet to trap any tars.

Residues were analyzed for carbon, hydrogen, and nitrogen using a Perkin-Elmer Model 240 elemental analyzer. Residues were allowed to cool in the flowing gas stream and quickly transferred to sealed sample containers. Prior to CHN analysis, samples were weighed on a Cahn Gram Electrobalance, Model

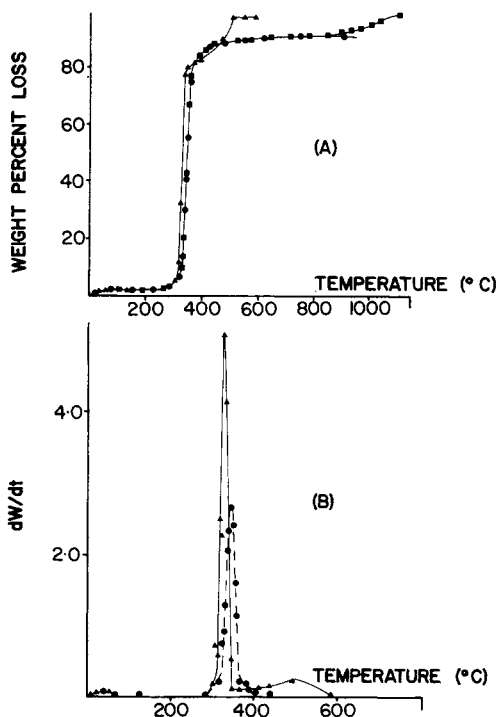


Fig. 2. TG curves (A) and DTG plots (B) for cellulose in nitrogen (●), in air (▲), and in nitrogen + H_2O (■).

G, which indicated no appreciable increase in sample weight. The results of the analyses were extremely reproducible.

RESULTS

Dynamic Thermogravimetry

The TG curve for cellulose in flowing nitrogen, Figure 2, was very similar to that obtained by Dollimore and Holt³—an initial 3% loss from 50° to 100°C followed by a plateau region to 290°C and a rapid weight loss beginning at 300°C

TABLE I
Kinetic Parameters for the Pyrolysis of Cellulose

Condition	T, °C	Rate constant, $\times 10^{-2}/\text{min}$	T_c , $\times 10^3 \text{ K}^{-1}$	A, min^{-1}	E_a , kJ/mole	Slope $\ln[-\ln(1-\alpha)]$ vs $\ln t$
First Stage in Nitrogen ($k = k_a$)	298	27.9 \pm 3.6				—
	305	52.2 \pm 8.2	17.89 \pm 5.06			—
	317	99.4 \pm 5.0		1.28 $\times 10^{13}$		—
	332	156.3 \pm 23.0			149	—
	341	301				—
First Stage in Air	275	16.6 \pm 5.0				—
	284	30.8 \pm 5.8	16.43 \pm 4.44			—
	311	95.8 \pm 6.1		1.82 $\times 10^{12}$		—
	326	238.0 \times 88.0			137	—
Second Stage Nitrogen ($k = k_b$)	298	0.45 \pm 0.03				—
	305	0.71 \pm 0.06	25.52 \pm 2.54			—
	317	1.98 \pm 0.34		1.13 $\times 10^{17}$		—
	332	5.89 \pm 0.16			212	—
	341	9.41 \pm 0.86				—
Second Stage in Air	275	0.80 \pm 0.03				—
	284	1.40 \pm 0.10	19.55 \pm 6.75			—
	311	9.26 \pm 0.64		2.55 $\times 10^{13}$		—
	326	14.64 \pm 2.62			163	—
Second Stage in Nitrogen Nitrogen ($k = k_c$)	298	1.23 \pm 0.09				1.13 \pm 0.07
	305	1.74 \pm 0.06	26.47 \pm 3.66			1.00 \pm 0.03
	317	4.63 \pm 0.45		1.51 $\times 10^{18}$		1.07 \pm 0.10
	332	16.79 \pm 0.82			220	1.24 \pm 0.03
	341	27.33 \pm 1.91				1.50 \pm 0.07
Second Stage in Air	275	1.77 \pm 0.12				1.16 \pm 0.06
	284	3.15 \pm 0.31	21.81 \pm 4.78			1.06 \pm 0.07
	311	23.97 \pm 1.69		3.43 $\times 10^{15}$		1.32 \pm 0.13
	326	47.07 \pm 14.45			181	1.71 \pm 0.25
DTG in Nitrogen	284	—	29.8 \pm 4.6			—
	to 337	—		2.61 $\times 10^{20}$	248	—
DTG in Air	290	—	41.3 \pm 3.5			—
	to 360	—		1.93 $\times 10^{29}$	343	—

to yield 92% weight loss at 1000°C. Results in air were identical below 290°C. The major weight loss began at 300°C and increased rapidly to 80% loss at 340°C. A second region occurred from 350° to 500°C to leave 2% residue at 1000°C. Below 830°C, the TG curve obtained in nitrogen plus water vapor (21.7 torr partial pressure) was identical to that found in dry nitrogen. At this temperature, a second weight loss region began and produced 98% loss at 1080°C.

First derivative plots (DTG), Figure 2, indicated that the maximum rate of cellulose pyrolysis in nitrogen (2.60 %/min) occurred at 350°C, while the maximum rate in air (5.00 %/min) occurred at 330°C.

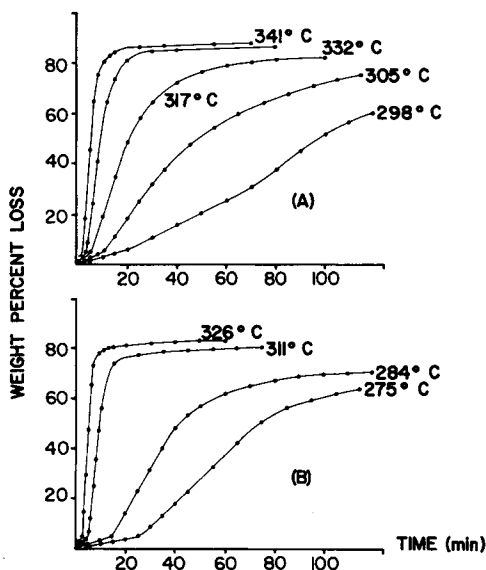


Fig. 3. Thermal decomposition of cellulose in nitrogen (A) and in air (B).

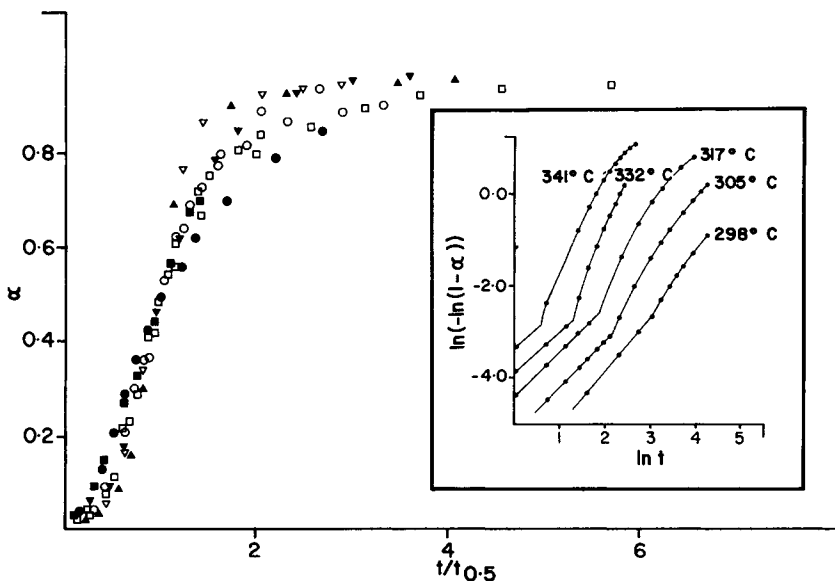


Fig. 4. Reduced time plot of the isothermal decomposition of cellulose. Insert: Plot of $\ln[-\ln(1-\alpha)]$ vs $\ln t$ for cellulose pyrolysis in nitrogen.

Kinetic parameters for decomposition were determined using the procedure described by Tang,¹² which assumes a first-order reaction where the rate of weight percent loss with time was evaluated as $(dW/dT)(dT/dt)$ and the rate constant k was determined from the expression

$$dW/dt = k(W_f - W_t) \quad (1)$$

where W_f is the final weight percent loss and W_t is the weight percent loss at time t . Arrhenius plots gave rise to approximate straight lines. The kinetic parameters are given in Table I.

Isothermal Pyrolysis of Cellulose

Plots of weight percent loss versus time, Figure 3, showed linear response to approximately 5% loss, followed by a rapid loss and subsequently by a slow approach to constant weight. At all temperatures this final loss was 88% in nitrogen and 84% in air. An instantaneous weight loss, from 1.20 to 0.35 mg, was observed with all samples to decrease as the treatment temperature was increased. Similar effects have been observed elsewhere^{2,11} and are probably related to buoyancy and gas/solid equilibrium phenomena. The initial specimen weight was obtained by an extrapolation of the first linear region of weight loss to zero time.

When plotted in the standard kinetic form as degree of decomposition α against reduced time $t/t_{0.5}$, the data showed significant scatter, Figure 4. The general shape of the curves, however, resembled those which would be described by an Avrami-Erofeev^{13,14} nucleation and growth expression of the type

$$[-\ln(1 - \alpha)]^{1/n} = kt \quad (2)$$

where n is 2 or 3.

Plots of $\ln[-\ln(1 - \alpha)]$ versus $\ln t$ were therefore constructed, Figure 4, to verify the possible use of such an expression. These plots clearly indicated an initial linear region at values of $\alpha < 0.05$, followed by a gentle curve over the region of α from 0.05 to 0.85. Hence, kinetic parameters were not derived from eq. (2). In an alternative approach, cellulose pyrolysis was described as two processes: an initial process of constant rate of loss, and a second which produced the major weight loss.

Tests showed that kinetic parameters could be obtained for the initial region using a zero-order rate expression:

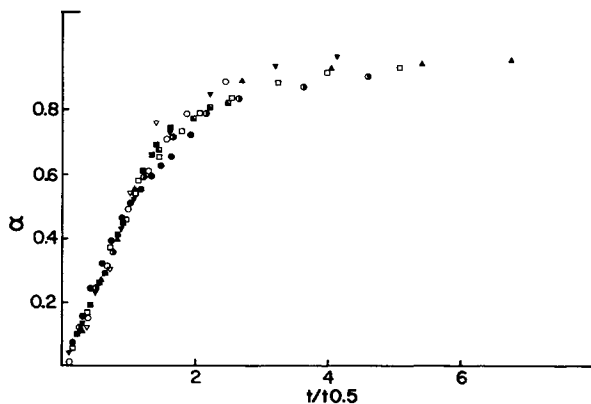


Fig. 5. Reduced time plot of the isothermal decomposition of cellulose, second stage.

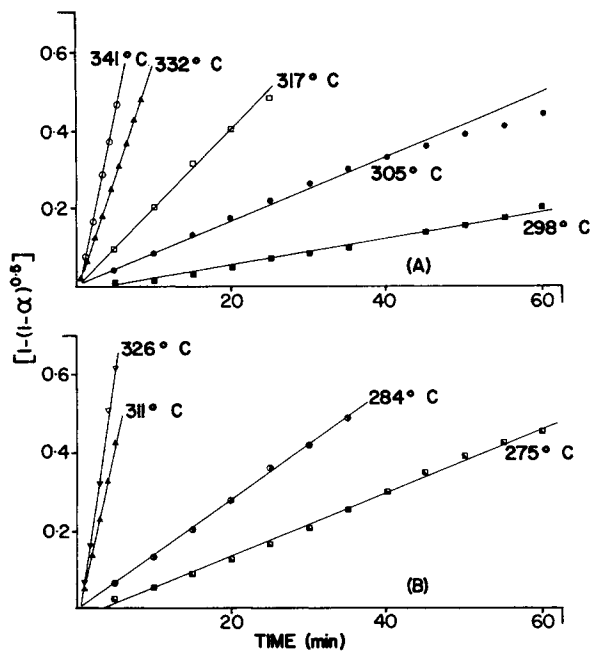


Fig. 6. Kinetics of decomposition of cellulose in nitrogen (A) and in air (B).

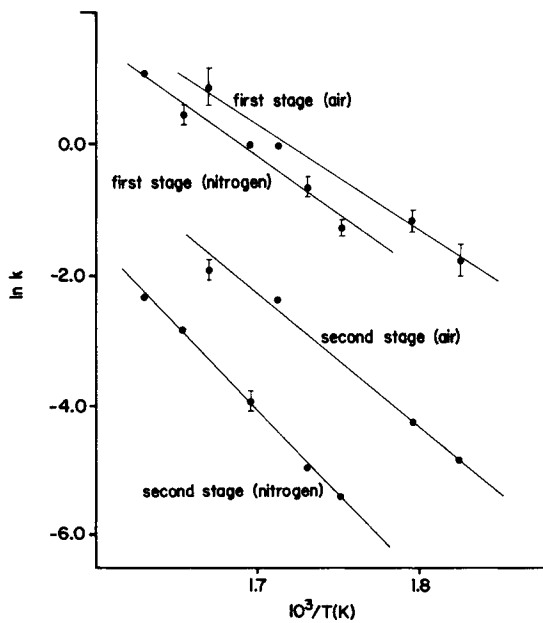


Fig. 7. Arrhenius-type plot for the thermal decomposition of cellulose.

$$dW/dt = k_a \quad (3)$$

where W is the weight percent loss at time t . Graphs of weight percent loss versus time gave straight lines of slope k_a in this region, and Arrhenius plots gave the kinetic parameters which are summarized in Table I. The initial loss was real and not simply a temperature effect since the sample temperature reached the operating temperature rapidly.

Reduced time plots for the second region of cellulose pyrolysis were obtained by considering the point of inflection on the weight percent loss-time curves as the origin. These plots exhibit significantly less scatter and were identical for results in both air and nitrogen, Figure 5, and the data were observed to fit the curve derived from the expression

$$1 - (1 - \alpha)^{0.5} = (u/r)t \quad (4)$$

which describes a reaction rate controlled by the movement of an interface at constant velocity u for a disk or cylinder of radius r .¹⁵ The rate constant k_b , given by u/r , was obtained from the slope of the linear plots of $1 - (1 - \alpha)^{0.5}$ versus time, Figure 6. Values for the temperature effect, line gradient T_c , and preexponential factor A were derived from Arrhenius plots, Figure 7, and are given in Table I.

The second region of cellulose pyrolysis may also be approximated by the usual first-order expression applicable to unimolecular decay processes:

$$-\ln(1 - \alpha) = k_c t \quad (5)$$

Plots of $-\ln(1 - \alpha)$ versus $\ln t$ produced reasonably straight lines of slope 1.0, Table I. When plotted in the standard kinetic form, the data more closely resembled the reduced time curve derived from eq. (4). The numerical values obtained for T_c were $25.52 \times 10^3 \text{ K}^{-1}$, eq. (4), and $26.47 \times 10^3 \text{ K}^{-1}$, eq. (5), for pyrolysis in nitrogen; and $19.55 \times 10^3 \text{ K}^{-1}$, eq. (4), and $21.81 \times 10^3 \text{ K}^{-1}$, eq. (5), for pyrolysis in air. The numerical results for T_c are within the error estimate for a 95% confidence interval for the two kinetic expressions as indicated in Table I.

The results from Figure 3 were also plotted as "rate of weight percent loss"

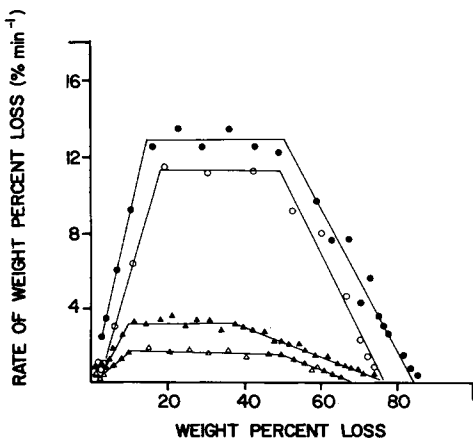


Fig. 8. Rates of cellulose decomposition: (●) 341°C in nitrogen; (▲) 317°C in nitrogen; (○) 311°C in air; (△) 284°C in air.



Fig. 9. Scanning electron micrographs of cellulose, scale $40\ \mu$ (A); and cellulose residues at 264°C in air, scale $20\ \mu$ (B), at 284°C in air, scale $40\ \mu$ (C), 298°C in air, scale $20\ \mu$ (D), 326°C in air, scale $20\ \mu$ (E), and 341°C in nitrogen, scale $40\ \mu$ (F).

vs "weight percent loss," Figure 8. The latter stages of these plots were very similar to those obtained for various cellulose samples by Madorsky, Hart, and Straus.^{7,16} An initial region of constant rate of loss, up to 5%, was followed by a region of constantly increasing rate up to 10–20% weight loss. An apparently constant rate of weight loss then occurred up to 50% loss, whence the rate began to decrease to the termination point. Hence, as noted previously by Lipska and Parker,² the "apparent activation energy" for cellulose pyrolysis will depend on the region of weight loss under consideration. The results shown in Figure 8 do not entirely obey the expected relationship for any single kinetic model over the whole region.

The values for the preexponential factor A (min^{-1}) and "apparent activation energy" E_a (kJ/mole) for cellulose pyrolysis in this and earlier studies fit the kinetic compensation effect equation

$$\ln A = 0.2E_a - 1.86 \quad (6)$$

which was shown previously to apply to the kinetics of pyrolysis of a number of wood products.¹ In all cases, the value for E_a has been evaluated as the slope of the Arrhenius plot (T_c) times the gas constant (R).

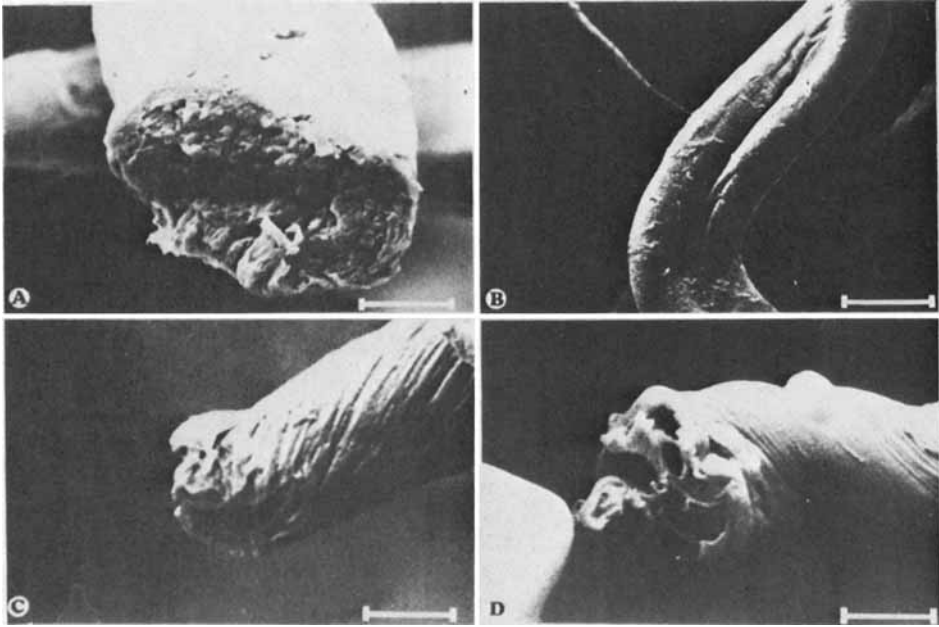


Fig. 10. Scanning electron micrographs of cellulose, scale $10\ \mu$ (A); and scale $20\ \mu$ (B); and cellulose residues at 326°C in air, scale $4\ \mu$ (C), and at 341°C in nitrogen, scale $4\ \mu$ (D).

Surface Areas

The surface area of the native cellulose powder was $0.8\ \text{m}^2/\text{g}$. The surface areas of the residues obtained from pyrolysis in nitrogen at 332°C and air at 326°C were 29.8 and $5.1\ \text{m}^2/\text{g}$, respectively. If it is assumed that the original cellulose does not undergo an increase in surface area per particle and that the residue contains more particles per gram due to an 85% reduction in weight, then the expected surface area becomes $(0.8)(100/15)$, or $5.3\ \text{m}^2/\text{g}$. Thus, it is apparent that cellulose pyrolysis in nitrogen produces a much larger increase in residue surface area than anticipated on this basis, while pyrolysis in air has little or no effect.

Scanning Electron Microscopy

The cellulose powder used in the present study consisted of long cylindrical fibers which appeared porous along the major axis. As shown in Figures 9 and 10, heat treatment produced a twisting of the original fibers with the production of some fractures perpendicular to the fiber axis at $<300^\circ\text{C}$. At higher temperatures, some fiber ends appear to "unravel," not unlike an end section of multistrand rope. The twisted-ribbon form of the fibers appears to increase with increase in heat treatment temperature. The fibers are approximately $23\ \mu$ wide and $11\ \mu$ thick.

Manley¹⁸ has described the basic morphologic unit of cellulose, the protofibril, as a ribbon which is pleated upon itself to give a zigzag structure of rectangular cross section, $35 \times 20\ \text{\AA}$, while cellulose fibrils have been considered to be cylindrical, $100\ \text{\AA}$ in diameter.³

TABLE II
Gaseous Product Analysis

Condition	Temperature, °C	Mole ratio		
		H ₂ /CO	CO ₂ /CO	CH ₄ /CO
Helium	250	7.1	2.1	—
	275	5.7	3.1	—
	300	1.9	3.5	CH ₄ (trace)
	350	1.6	2.7	0.02
Helium/Oxygen	250	—	6.1	—
	270	—	2.2	—
	300	—	2.2	—
	350	—	2.8	—

Gaseous Product Analysis

Gas analysis studies in both helium and helium/oxygen atmospheres indicated that at temperatures below 250°C, the only gaseous product was H₂O. It was observed that the major gaseous product of cellulose pyrolysis was H₂O at all temperatures. In helium, pyrolysis at higher temperatures produced H₂O, CO₂, CO, CH₄, and H₂, however, CH₄ was not detected below 300°C. Pyrolysis of cellulose in an oxidizing atmosphere produced mainly H₂O, CO₂, and CO, which may reflect the gaseous oxidation of any primary products. The relative mole fractions of the gases were calibrated from a known sample and, with the exception of H₂O, are presented relative to CO in Table II.

Residue Analysis

Isothermal pyrolysis of cellulose in nitrogen from 298° to 341°C produced a constant amount of residue (12%), with the elemental analysis 73.47% C, 3.56% H, and 22.97% O. Pyrolysis in air from 275° to 326°C produced 18% residue, with elemental analysis 59.37% C, 1.72% H, and 38.91% O. (The amount of oxygen present in the residues was estimated by difference.)

These data were also analyzed by plotting the atomic H/C ratio against the atomic O/C ratio along with results obtained from the pyrolysis of other wood products.¹⁷ The comparison indicated that residues from cellulose pyrolysis resembled those from wood pyrolysis and that, in nitrogen, the major reaction producing the residue was dehydration.

DISCUSSION

Physical Mechanism of Cellulose Pyrolysis

The results of weight-change determinations on cellulose powder clearly indicate that at least two distinct processes occur during the pyrolysis of cellulose even in the presence of oxygen, which accelerates the weight loss.

The first observable process of pyrolysis has been described in terms of a zero-order reaction with respect to weight percent loss, in agreement with those investigators who have suggested that a zero-order dehydration reaction is likely to occur.^{9,20} It has been observed that cellulose undergoes a reduction in degree of polymerization (D.P.) to less than 200 during pyrolysis,^{5,20} with only a 3–6%

loss in weight,^{11,5} and this probably occurs by the transglycosylation mechanism proposed by Shafizadeh.²¹ Cleavage of the glycosidic groups is thought to produce anhydro sugars which then polymerize to some extent by condensation reactions and eventually lead to the formation of char. In the present study, the initial reaction proceeded to the same weight loss (5%) under all conditions. This is a discrete stage which is only observable until the second weight-loss process predominates.

The initial exothermic reaction in the pyrolysis of cellulose, observed by DTA,²² has been ascribed to rapid crosslinking in agreement with the chemical description of pyrolysis. This also explains the first weight loss region as the loss of water molecules through intra- and intermolecular dehydration reactions. The T_c values determined for the first weight-loss region, $17.16 \times 10^3 \text{ K}^{-1}$ in nitrogen and $16.43 \times 10^3 \text{ K}^{-1}$ in air, agree with those values found by other investigators for the first region of cellulose pyrolysis^{8,9,23} and are consistent with the observed decrease in D.P. with heat treatment.⁵

If only dehydration and condensation reactions occur, then only water should have been detected in the gaseous products. However, the gas analysis indicated that a number of products were evolved immediately on pyrolysis at temperatures above 250°C. A similar observation was made by Murphy.⁸ This suggests that the initial weight loss is not exclusively due to dehydration but that some decomposition of the bulk also takes place.

The electron micrographs, Figures 9 and 10, indicate that the surface of the cellulose fibers was not drastically altered by pyrolysis. In the native cellulose powder, the surface fibrils appear to be more dense than the interior, and it is possible that the surface layers have been altered somewhat by chemical pretreatment of the sample, as in the pulping process, and therefore might behave differently from the fiber interior. The surface, however, constitutes less than 3% of the total weight of the fiber and will not affect the weight loss results significantly.

The major weight loss occurs as a bulk reaction and is likely to involve the loss of low molecular weight fragments to give tars and decomposition of monomer units by dehydration, fission, and disproportionation reactions to give volatiles as described by Shafizadeh.²¹ An induction period for this second region, indicating the buildup of chemical species, is apparent from Figures 3 and 8.

The rate-controlling step in cellulose pyrolysis seems likely to be primarily associated with a chemical/physical equilibrium condition. According to the rate data, Figure 8, the second weight-loss stage proceeds in discrete steps: an induction period, a region of rapidly increasing rate, a region of constant rate, and a region of constantly decreasing rate. Thus, the second stage may be described as follows: (1) An induction period occurs in which there is a buildup in concentration of lower molecular weight molecules, followed by (2) a decomposition of monomer units in the fiber interior with a rapidly increasing rate; and, (3) at some point in the reactions, an equilibrium arises where the rate of formation of product is equal to the rate of removal, while (4) in the latter stages, the loss of weight is entirely transport controlled.

A plot of rate of weight percent loss versus weight percent loss for the dynamic thermogravimetric results indicated a gentle increase in rate with extent of reaction to a maximum at approximately 50%, followed by a gentle decrease in a pattern which is the same as that expected for a kinetic expression similar to eq

(2). This serves to indicate that in an increasing temperature environment, there is insufficient settling time for a chemical/physical equilibrium process to occur in contrast to the isothermal conditions.

Initially, cellulose pyrolysis is thought to involve a series of intermolecular dehydration reactions which eventually lead to the formation of char in agreement with the general model of Broido and Nelson¹⁹ and subsequent kinetic description by Broido.²⁴ The second process involves the formation of volatiles only and accounts for the major weight loss. The rate increase in the presence of oxygen can be explained if it is assumed that oxygen is free to enter the interior of the fibers where it accelerates radical reactions. The interactions of oxygen with the char-producing reactions could substitute oxygen molecules into the residue, thus reducing crosslinking which occurs under inert conditions to yield a porous char, and this would be consistent with the lower value of surface area obtained for the residue in the air experiments.

CONCLUSIONS

The pyrolysis of cellulose powder has been studied in both inert and oxidizing atmospheres; and while the mechanisms are similar, pyrolysis in air may be catalyzed by molecular oxygen in radical interactions. Pyrolysis is thought to occur by two discrete processes. One is observed in the early stages of pyrolysis for which the temperature effect as described by T_c , the gradient of the Arrhenius plot, was determined by a zero-order kinetic expression to be approximately $17.16 \times 10^3 \text{ K}^{-1}$ in both atmospheres.

The major decomposition process occurs in the fiber interior with a T_c value of $25.52 \times 10^3 \text{ K}^{-1}$ in nitrogen and $19.55 \times 10^3 \text{ K}^{-1}$ in air. The reaction kinetics were derived from a phase boundary model and could also be derived from a first-order rate law. Kinetic parameters obtained from isothermal and dynamic TG studies fit a compensation curve described previously for the decomposition of wood products.

The authors would like to thank the Ontario Ministry of the Environment for the fellowship (S.P.S.) and the assistantship (C.F.) awards.

References

1. C. Fairbridge, R. A. Ross, and P. Spooner, *Wood Sci. Technol.*, **9**, 257 (1975).
2. A. E. Lipska and W. J. Parker, *J. Appl. Polym. Sci.*, **10**, 1439 (1966).
3. D. Dollimore and B. Holt, *J. Polym. Sci. A2*, **11**, 1703 (1973).
4. P. K. Chatterjee and C. M. Conrad, *Text. Res. J.*, **36**, 487 (1966).
5. D. P. C. Fung, *Tappi*, **52**, 319 (1969).
6. M. V. Ramiah, *J. Appl. Polym. Sci.*, **14**, 1323 (1970).
7. S. L. Madorsky, V. E. Hart, and S. Straus, *J. Res. Natl. Bur. Stand., Res. Pap.*, **56**(6), 2685 (1956).
8. E. J. Murphy, *J. Polym. Sci.*, **58**, 649 (1962).
9. D. F. Arsenéau, *Canad. J. Chem.*, **49**, 632 (1971).
10. Y. Kumagai and T. Ohuchi, *Jpn. Wood Res. Soc. J.*, **20**, 381 (1974).
11. A. Basch and M. Lewin, *J. Polym. Sci., Polym. Chem. Ed.*, **11**, 3095 (1973).
12. W. K. Tang, *U.S. For. Serv., Res. Pap. FPL 71*, 1967, Forest Prod. Lab., Madison, Wisconsin.
13. M. Avrami, *J. Chem. Phys.*, **9**, 177 (1941).
14. B. V. Erofeev, *C.R. (Dokl.) Acad. Sci.*, **LII**(No. 6), 511 (1946).
15. J. H. Sharp, G. W. Brindley, and B. N. N. Achar, *J. Am. Ceram. Soc.*, **49**, 379 (1966).

16. S. L. Madorsky, V. E. Hart, and S. Straus, *J. Res. Natl. Bur. Stand., Res. Pap.*, **60**(4), 2853 (1958).
17. C. Fairbridge, M.Sc. Thesis, Lakehead University, 1976.
18. R. St. John Manley, *J. Polym. Sci. B*, **3**, 691 (1964); *J. Polym. Sci. A2*, **9**, 1025 (1971).
19. A. Broido and M. Nelson, *Combust. Flame*, **24**, 263 (1975).
20. M. Kosik, V. Luzakova, and V. Reiser, *Cellulose Chem., Technol.*, **6**, 589 (1972).
21. F. Shafizadeh, *J. Appl. Polym. Sci., Appl. Polym. Symp.*, **No. 28**, 153 (1975).
22. D. Dollimore and G. R. Heal, *Carbon*, **5**, 65 (1967).
23. W. K. Tang and W. K. Neill, *J. Polym. Sci. C*, **6**, 65 (1964).
24. A. Broido, Abstracts of Papers, 172nd ACS National Meeting, Division of Carbohydrate Chemistry, 1976, p. 107.

Received December 23, 1976

Revised February 8, 1977